

## Article

# A Comprehensive Investigation of BN and VC Reinforcements on the Properties of FSP AA6061 Composites

Essam B. Moustafa <sup>1,\*</sup>, Fathi Djouider <sup>2</sup>, Abdulsalam Alhawsawi <sup>2,3</sup>, Ezzat Elmoujarkach <sup>2</sup>,  
Essam Banoqitah <sup>2,3</sup> and Samah S. Mohamed <sup>4</sup>

<sup>1</sup> Mechanical Engineering Department, Faculty of Engineering, King Abdulaziz University, P.O. Box 80204, Jeddah 21589, Saudi Arabia

<sup>2</sup> Nuclear Department, Faculty of Engineering, King Abdulaziz University, P.O. Box 80204, Jeddah 21589, Saudi Arabia; fdjouider@kau.edu.sa (F.D.); ebanqitah@kau.edu.sa (E.B.)

<sup>3</sup> Center for Training & Radiation Prevention, King Abdulaziz University, P.O. Box 80204, Jeddah 21589, Saudi Arabia

<sup>4</sup> Mechanical Engineering Department, Shoubra Faculty of Engineering, Benha University, Cairo 11629, Egypt; samah.samir@feng.bu.edu.eg

\* Correspondence: abmostafa@kau.edu.sa

**Abstract:** This present study investigated the impact of incorporating boron nitride (BN) and vanadium carbide (VC) reinforcements on various properties of friction stir processed (FSP) AA6061 alloy composites, focusing specifically on grain structure, thermal conductivity, electrical conductivity, and compressive strength. The findings indicate that VC more effectively refines the grain structure of the AA6061 alloy during FSP compared to BN. The inclusion of BN particles in the metal matrix composites resulted in a decrease in both thermal and electrical conductivity. In contrast, the addition of VC particles led to an increase in both thermal and electrical conductivity. The AA6061/VC composite material exhibited the highest thermal conductivity among all composites tested. The electrical conductivity of the hybrid-composite AA6061/30%BN+70%VC showed a slight reduction, measuring only 2.8% lower than the base alloy AA6061. The mono-composite AA6061/VC exhibited a marginal decrease in thermal conductivity, with a measured value only 7.5% lower than the conventional alloy AA6061. However, the mono-composite AA6061/BN displayed a more significant decline, exhibiting a loss of 14.7% and 13.9% in electrical and thermal conductivity, respectively. The composite material comprising 30% BN and 70% VC reinforcement demonstrated the highest compressive strength compared to all other tested composites. The observed percentage enhancement in the mechanical properties of mono and hybrid composites, compared to the parent AA6061 alloy, ranged from 17.1% to 31.5%.

**Keywords:** FSP; mono composite; hybrid composite; compressive; microstructure; thermal and mechanical conductivity



**Citation:** Moustafa, E.B.; Djouider, F.; Alhawsawi, A.; Elmoujarkach, E.; Banoqitah, E.; Mohamed, S.S. A Comprehensive Investigation of BN and VC Reinforcements on the Properties of FSP AA6061 Composites. *Lubricants* **2023**, *11*, 507. <https://doi.org/10.3390/lubricants11120507>

Received: 6 November 2023

Revised: 26 November 2023

Accepted: 28 November 2023

Published: 30 November 2023



**Copyright:** © 2023 by the authors. Licensee MDPI, Basel, Switzerland. This article is an open access article distributed under the terms and conditions of the Creative Commons Attribution (CC BY) license (<https://creativecommons.org/licenses/by/4.0/>).

## 1. Introduction

The utilization of aluminum alloys is prevalent throughout various applications owing to their exceptional strength-to-weight ratio, elevated corrosion resistance, and commendable thermal and electrical conductivity. Nevertheless, certain materials' limited hardness and wear resistance may restrict their applicability in some contexts [1,2]. Integrating ceramic nanoparticles, such as VC, BN, SiC, GNP, BC, etc., into aluminum alloys through friction stir processing has significantly impacted the resulting composites' mechanical and thermal properties [3–7]. The utilization of ceramic reinforcements in AA6061 by Friction Stir Processing (FSP) has substantially improved its characteristics. In a study conducted by [8], it was shown that the incorporation of vanadium and niobium carbides resulted in enhanced mechanical and physical characteristics. These improvements

encompassed heightened compressive and yield stress, higher hardness, and a lowered coefficient of thermal expansion. Hynes et al. [9] documented comparable results with boron carbide, emphasizing improved mechanical properties and wear resistance. In addition, Sharma et al. [10] provided more evidence to support the efficacy of hybrid composites, highlighting the enhanced tribological performance achieved by incorporating MoS<sub>2</sub> particles. In a study conducted by [11], the authors investigated the effects of ZrO<sub>2</sub>/GNP and B<sub>4</sub>C/GNP reinforcements on the mechanical properties of the composite matrices. The results indicated that both reinforcements led to a considerable increase in hardness and wear resistance. The research, as mentioned earlier, collectively demonstrates the potential of using ceramic reinforcements, such as boron nitride and vanadium carbide, to customize the characteristics of AA6061 according to individual needs.

The utilization of BN and VC nanoparticles as reinforcements for aluminum alloys has gained attention due to their distinctive properties, including increased hardness, enhanced thermal conductivity, and outstanding electrical conductivity [12]. The mobility of dislocations is hindered by these entities, thereby augmenting the strength and toughness of the material. Additionally, the incorporation of ceramic particles can hinder the advancement of cracks due to their function as stress concentrators [13,14]. The solid-state processing technique, commonly called FSP, can produce aluminum alloy composites demonstrating an evenly dispersed configuration of reinforcements inside the matrix [15–17]. BN impacts the mechanical characteristics of aluminum. Thus, incorporating BN particles into the aluminum matrix reinforces the composite material, resulting in enhanced strength and stiffness properties [18]. This phenomenon can substantially enhance tensile strength, yield strength, and hardness [19]. Boron nitride (BN) particles have been found to significantly affect the thermal and electrical conductivity of aluminum alloy composites [20]. The composite's thermal conductivity increases with the BN particles' size. The enhanced heat transfer efficiency of bigger BN particles can be attributed to their increased surface area. Al–BN composites with a cBN particle size of 20 μm demonstrated superior hardness, elastic modulus, densification, corrosion resistance, and pitting corrosion resistance compared to other composites and pure aluminum. This improvement is attributed to the better stress drive in the matrix and the absence of chemical reactions or interfacial phases at 550 °C. These findings suggest the potential of Al–BN composites as promising materials for various applications [21].

Nevertheless, it should be noted that including bigger BN particles in the composite material may decrease its electrical conductivity. Hence, this feature can prove advantageous in scenarios where efficient heat dissipation is critical [22]. In a research conducted by [23], the investigation focused on analyzing the influence of BN particle content on the microstructure and mechanical characteristics of (FSP) AA6061-T6/BN composites. The study's findings indicated that incorporating BN particles substantially enhanced the composite material's hardness, tensile strength, and yield strength. As mentioned earlier, the investigation demonstrates that incorporating BN ceramic particles into aluminum-based composites notably enhances their mechanical properties [24]. The observed enhancement can be ascribed to the reinforcing influence of the BN particles, which contribute to heightened strength and stiffness inside the composite matrix [25]. R. Palanivel et al. [26] investigated the effects of boron nitride nanoparticles on the microstructure and wear properties of AA6082/TiB<sub>2</sub> hybrid aluminum composites fabricated through friction stir processing. The results showed that TiB<sub>2</sub> and BN particles were evenly distributed throughout the stir zone, decreasing grain size from 39.4 μm to 6.6 μm, with effective bonding between the aluminum matrix and TiB<sub>2</sub> and BN particles. The investigation of the influence of vanadium carbide VC on the mechanical, thermal, and electrical characteristics of aluminum composite matrices represents a significant focal point within the realm of materials science research [27,28]. The properties of the aluminum matrix can be greatly modified, and its overall performance can be improved by the incorporation of vanadium carbide particles [8]. The influence of VC particles on the microstructural characteristics of aluminum alloy composites is contingent upon various elements, encompassing the size of

the particles, their presence within the composite, and the employed processing technique. Typically, VC particles tend to enhance the grain size refinement inside the aluminum matrix and facilitate the dispersion of the reinforcement particles [29,30]. Previous studies have investigated the impact of BN and VC reinforcements on the properties of AA6061 alloy composites. However, these studies have primarily focused on the effect of individual reinforcements on specific properties. This study addresses the existing knowledge gap by investigating the synergistic effects of incorporating both BN and VC reinforcements on the grain structure, thermal conductivity, electrical conductivity, and compressive strength of FSPed AA6061 alloy composites. This study's novelty lies in its comprehensive approach to evaluating the impact of BN and VC reinforcements, both individually and in combination, on a range of critical properties of AA6061 alloy composites. The findings of this study will provide valuable insights into designing and developing high-performance aluminum alloys for various applications. In the current investigation, the effects of incorporating BN and VC nanoparticles into AA6061 aluminum alloy on the new composite's hardness, microstructure, thermal, and electrical properties regarding different mono- and hybrid-composites volume fractions. The combination of the two different types of reinforcement particles, BN and VC, into a single composite, has not been undertaken before in the previous literature. In particular, incorporating nano-sized boron nitride particles and micron-sized vanadium carbide particles influences the characteristics of the composite formed by the FSP method.

## 2. Materials and Experimental Procedures

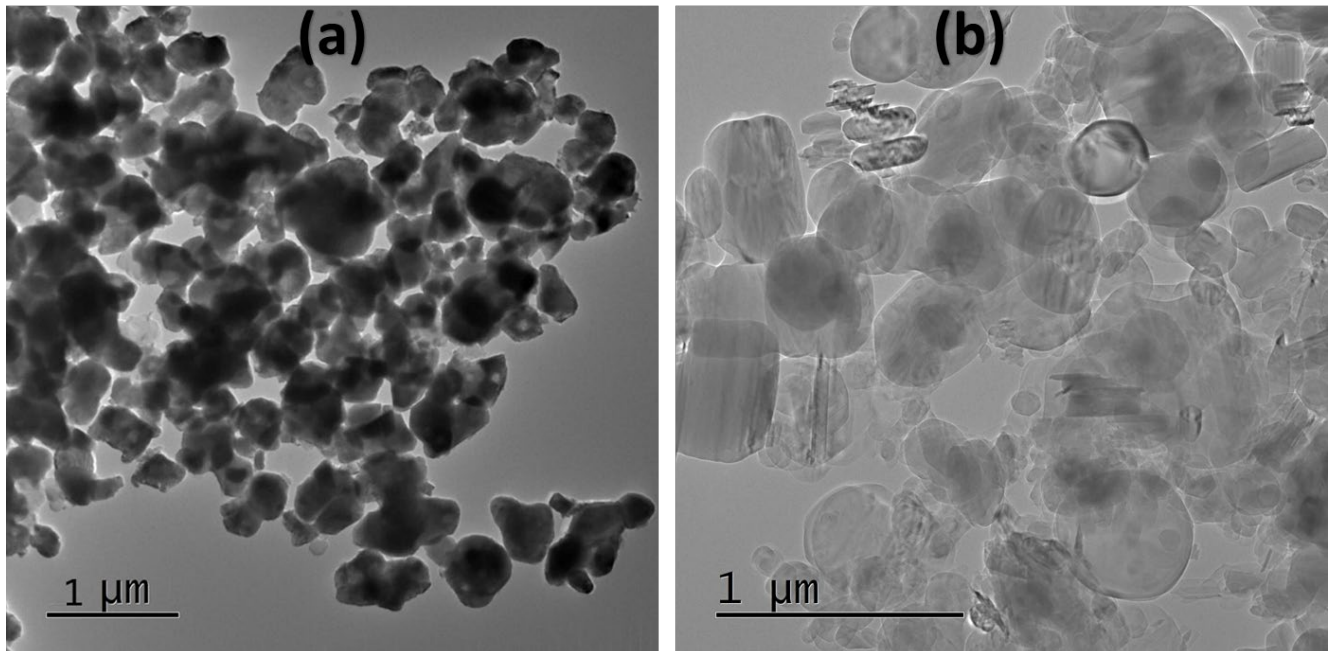
### 2.1. Materials

The choice of commercial alloy AA6061 rolled plates as the fundamental matrix in this investigation was motivated by their extensive range of practical uses and chemical composition (see Table 1). Steel K110 is typically used as a (FSP) tool, with the pin shape specifically engineered to possess a taper triangle tool geometry. The surface of the basic alloy was reinforced with BN nanoparticles and VC microparticles, which served as nanoceramic reinforcements. The reinforcing nanoparticles were selected based on their ability to enhance wear resistance and hardness characteristics. The visual characteristics of the reinforcement particles in the transmission electron microscopy (TEM) images were remarkably similar. Figure 1a displays the VC microparticles, which had an average particle size of  $1 \pm 0.21 \mu\text{m}$ , while Figure 1b shows the BN nanoparticles with an average particle size of  $600 \pm 48 \text{ nm}$ . The VC microparticles exhibited a diminutive size and had a sleek surface, while the BN nanoparticles displayed a substantial size and a smooth surface. The resemblance in physical characteristics between these two particle types can be attributed to their same chemical composition and crystal structure. Both VC and BN are characterized by their high hardness and inertness, rendering them very suitable for use as reinforcement particles in composite materials.

Nevertheless, the increased dimensions of the BN nanoparticles may confer certain benefits compared to the VC microparticles. For instance, it has been observed that BN nanoparticles exhibit enhanced efficacy in impeding crack propagation inside a composite material, leading to an improvement in the overall toughness of said composite. The hybrid composites were manufactured with a uniform volume content ratio. As a result, the first hybrid composite consisted of 30% VC and 70% BN, while the second hybrid composite comprised 70% VC and 30% BN. It has been established that combining two types of reinforcement can lead to a more effective strengthening effect than the individual reinforcement particles alone.

**Table 1.** Chemical composition of the commercial wrought AA6061 alloy.

Element	Mg	Mn	Si	Fe	Cu	Zn	Other	AL
(wt)%	0.69	0.34	0.41	0.83	0.25	0.19	0.12	remain

**Figure 1.** The TEM images of the reinforcement particles. (a) VC microparticles, (b) BN nanoparticles.

## 2.2. Fabrication Process

The fabrication of the nanocomposite surface on aluminum plates involved the utilization of FSP. Before this, the aluminum plates were prepared and cut using a milling machine to create a series of holes arranged in a linear pattern, as depicted in Figure 2a. The insertion of reinforcement nanoparticles into the cavity of the holes was carried out through two distinct scenarios. The first scenario used a pure mono composite consisting of AA6061/BN and AA6061/VC. The second scenario investigated the influence of varying the percentage of reinforcement particles within the hybrid-composite matrix. The ceramic particle hybrids were thoroughly blended and agitated before being incorporated into the underlying matrix. In addition, the hybrid materials were evenly distributed and incorporated into the mixture before being inserted into the holes of the basic matrix. Figure 2b depicts the fabrication process of the nanocomposite surface using the FSP method. The procedure was executed using an automated milling machine under the specified parameters: a rotary tool speed of 1125 revolutions per minute (rpm); a linear moving speed rate of 30 mm per minute (mm/min); and a fixed tilt angle of 3° degree. The tool has a shoulder diameter of 25 mm and a special pin profile based on a triangular polygon profile with chamfered corners and 6 mm depth. The triangular polygon profile is a common choice for FSP tools, providing good penetration and weld quality. The chamfered corners help to reduce stress concentrations and improve the fatigue life of the tool (Figure 3).

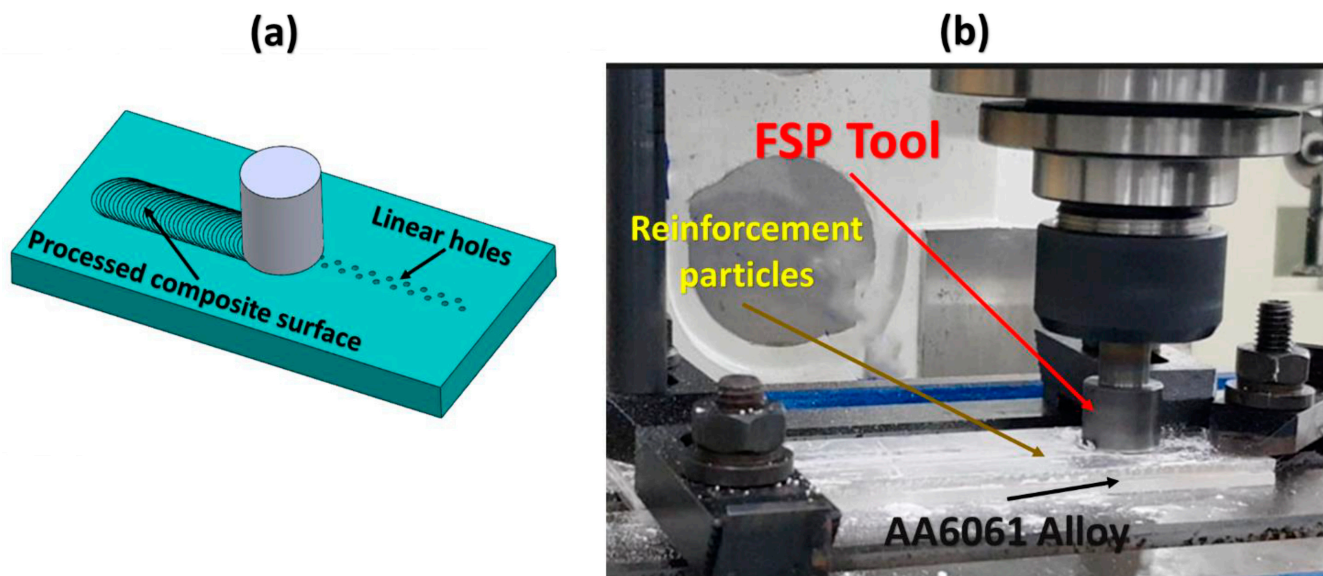


**Figure 2.** Fabrication process of the composite surface. (a) Hole design, (b) FSP process using a milling machine.

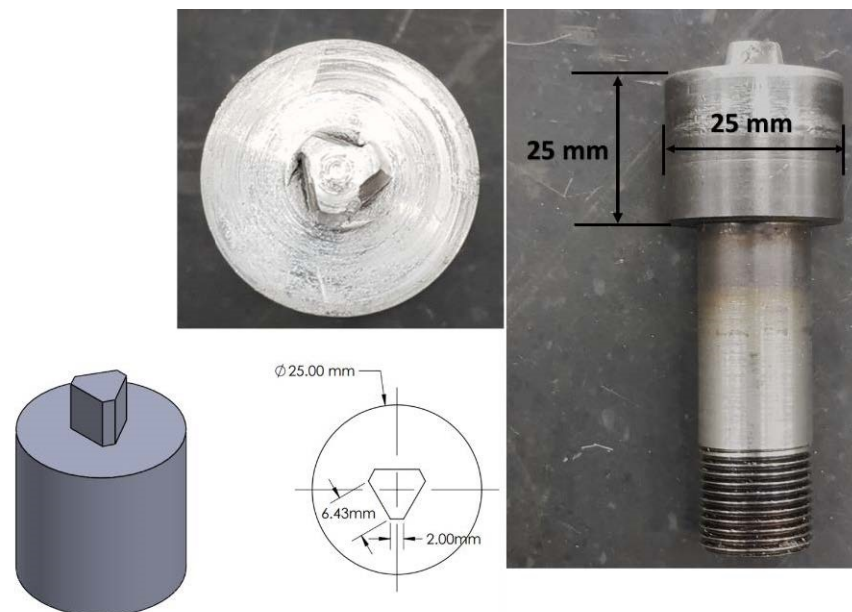


**Figure 3.** Typical FSP tool design.

### 2.3. Characterization and Tests

#### 2.3.1. Microstructure Examination

The FSPed surfaces' microstructure was examined using optical microscopy (OM) and scanning electron microscopy (SEM). The (OM) was conducted utilizing an Olympus BX51 microscope manufactured in the United States to understand the microstructure comprehensively. This experimental setup was utilized to capture high-resolution microstructure images and quantify individual grain sizes. The grain size of the FSPed samples was measured using the linear intercept method. For this method, a series of lines were drawn across the microstructure image, and the number of grain boundaries intersected by each line was counted [31]. The average grain size was then calculated by dividing the total number of grain boundaries by the total length of lines drawn.

$$\text{Grain size } (\mu\text{m}) = 2L/n \quad (1)$$

where  $L$  is the average length of the intercepts ( $\mu\text{m}$ ), and  $n$  is the number of intercepts counted.

### 2.3.2. Mechanical Property

A compression test was conducted on rectangular cross-section specimens of 4 mm and 8 mm and a length of  $20.00 \pm 0.20$  mm using a 300 kN capacity Universal Testing Machine (UTM) model (SANS: CMT2505, Sansi Yongheng Technology (Zhejiang, China) Co., Ltd., Ningbo, China) in accordance with the ASTM E9 standard. Before conducting the compression test, the cast specimens underwent a machining process using a lathe machine to rectify any deviations in the parallelism and smoothness of their flat surfaces. A face machining operation achieved this. Subsequently, the specimens were positioned amidst flat compression plates. The testing apparatus was configured in a displacement-control arrangement, where the cross-headed vertical speed was set at 1 mm/min. Three samples were subjected to testing, with each sample being tested many times. The resulting data were used to calculate average ultimate compressive strength (UCS) values.

### 2.3.3. Thermal Conductivity

Thermal conductivity was measured using the Armfield Linear Heat Conduction instrument, which utilizes thermocouples to ascertain the temperature distribution throughout a given specimen. The apparatus comprised a specimen holder, a heating element, and a sequence of thermocouples, as demonstrated in the previous work [32]. The sample was positioned within the sample holder, and thermal energy was delivered to one end of the sample using a heater. The temperature at several locations along the sample was measured using thermocouples.

$$Q = k * A * (\Delta T / \Delta x) \quad (2)$$

where  $Q$  is the heat flux ( $\text{W}/\text{m}^2$ );  $k$  is the thermal conductivity ( $\text{W}/\text{mK}$ );  $A$  is the cross-sectional area of the sample ( $\text{m}^2$ );  $\Delta T$  is the temperature difference between the two ends of the sample (K);  $\Delta x$  is the distance between the two thermocouples (m).

The determination of heat flux, denoted as  $Q$ , involves the measurement of the power input applied to the heater, which is subsequently divided by the cross-sectional area of the sample. The temperature difference, denoted as  $\Delta T$ , can be determined by measuring the temperature using two thermocouples. The value of  $\Delta x$ , representing the distance between the two thermocouples, can be determined based on the sample's geometry and the specific positioning of the thermocouples. The thermal conductivity can be determined by employing the given equation, which involves the known variables  $Q$ ,  $\Delta T$ , and  $\Delta x$ . The equation can be expressed as:

$$k = Q * \Delta x / A * \Delta T \quad (3)$$

### 2.3.4. Electrical Conductivity

The produced nanocomposites' electrical conductivity ( $\sigma$ ) was evaluated at 30 °C, utilizing a Keithley 6517B system. The Keithley 6517B is a precision electrometer that accurately measures electrical conductivity across a broad spectrum of magnitudes. The electrical conductivity measurements were conducted on at least five samples for each nanocomposite formulation.

$$\sigma = 1 / R * A \quad (4)$$

where  $R$  and  $A$  are the electrical resistance and the surface area of the specimen, respectively.

## 3. Results and Discussions

### 3.1. Microstructure Observation

Figure 4 depicts the effects of reinforcements on optical micrographs of AA6061 aluminum alloy taken from several sections before and after (FSP). The initial microstructure of AA6061 aluminum alloy consisted of elongated grains in a uniaxial direction (Figure 4a). FSP resulted in a significant alteration in the microstructure, with the presence of three

distinct zones: nugget or stirred zone (SZ); thermomechanically affected zone (TMAZ); and heat-affected zone (HAZ) (Figure 4b,c). FSP generates friction and significant plastic deformation, leading to heat generation in the SZ and the subsequent development of a dynamically recrystallized microstructure [33,34]. This explains the presence of increasingly homogeneous, equiaxed refined grains in the HAZ compared to the parent material [35]. Additionally, it was observed that the thermomechanically affected zone (TMAZ) and heat-affected zone (HAZ) exhibited narrow dimensions following (FSP) at a rotational speed of 1125 (RPM) and traverse rate of 30 (mm/min). However, using various reinforcing nanoceramics in FSP with either mono or hybrid reinforcements decreased the effectiveness of grain size reduction, suggesting that the nanoceramics act as grain refiners.

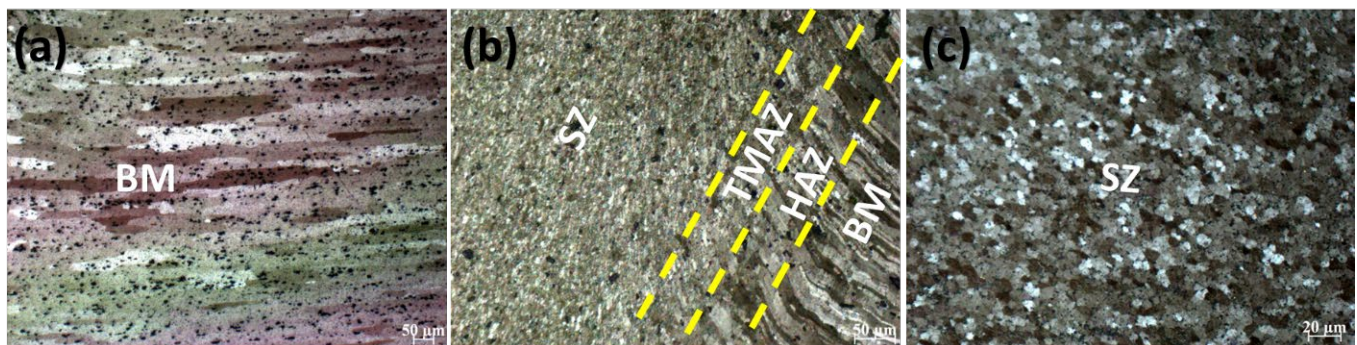


**Figure 4.** Optical microstructure images of the FSPed sample. (a) AA6061 base metal (BM), (b) mixed region of the stirred zone (SZ), thermomechanical affected zone (TMAZ), heat affected zone (HAZ), and base metal (BM) for AA6061 FSPed, (c) refined microstructure inside a stirred zone.

The base metal exhibited an average grain size of 210  $\mu\text{m}$ , accompanied by an aspect ratio of 20:8. It was observed that the average grain size within the stirred zone (SZ) exhibited a reduction to 18  $\mu\text{m}$ , accompanied by the presence of virtually equiaxed grains. The average grain sizes in the solidified zone (SZ) for the mono-composite vanadium carbide (VC), boron nitride (BN), and hybrid-composite (AA6061/30%BN+70%VC and AA6061/70%BN+30%VC) were measured to be 14 and 17  $\mu\text{m}$ , respectively. Table 2, shows the Statistical analysis showed a statistically significant difference in the average grain size of the different composite samples (Figure 5). The hybrid composites with fewer BN particles had the smallest grain size (AA 6061/30%BN+70%VC and AA 6061/50%BN+50%VC) apart from the mono-composite AA6061/30%VC. There are several potential explanations as to why (VC) demonstrates a greater capacity for refining the grain structure of the aluminum AA6061 alloy during (FSP) compared to (BN). Hence, it exhibited lower thermal stability compared to (VC). During FSP, the material undergoes exposure to elevated temperatures. (VC) exhibited greater deformation resistance at elevated temperatures than (BN), enhancing its ability to maintain structural integrity and serve as an effective pinning site for grain boundaries. (VC) exhibited a comparatively elevated melting point compared to (BN). This implies that adding VC can effectively mitigate the occurrence of grain boundary melting and subsequent recrystallization during (FSP). The chemical reactivity of the (VC) with aluminum was greater than that of BN. This phenomenon implies that (VC) can establish a more robust interfacial connection with the aluminum matrix, enhancing its efficacy in impeding the motion of grain boundaries.

**Table 2.** Average grain size and aspect ratio of AA6061 composites.

Samples	Avg Grain Size $\mu\text{m}$	Aspect Ratio %
Base AA 6061	$210 \pm 12$	32
FSPed AA 6061	$18 \pm 2$	81
AA6061/BN	$19 \pm 1.5$	79
AA6061/VC	$12 \pm 1.7$	89
AA 6061/50%BN+50%VC	$16 \pm 1.9$	85
AA 6061/30%BN+70%VC	$14 \pm 1.3$	82
AA 6061/70%BN+30%VC	$17 \pm 1.5$	83

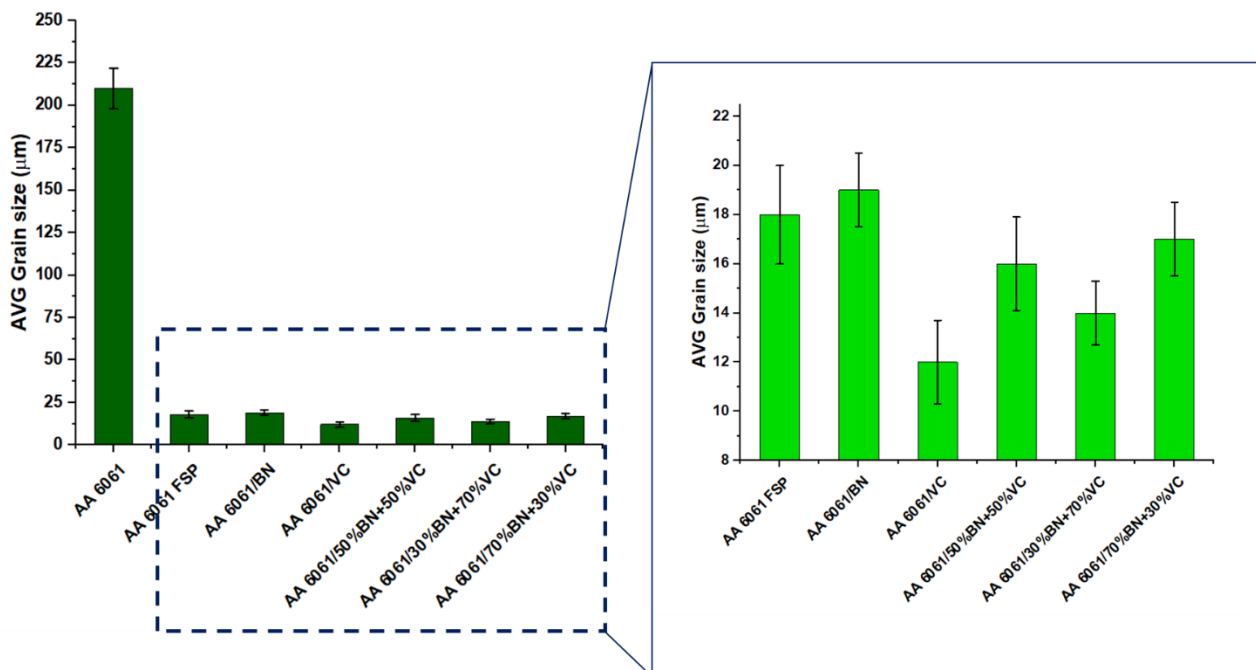
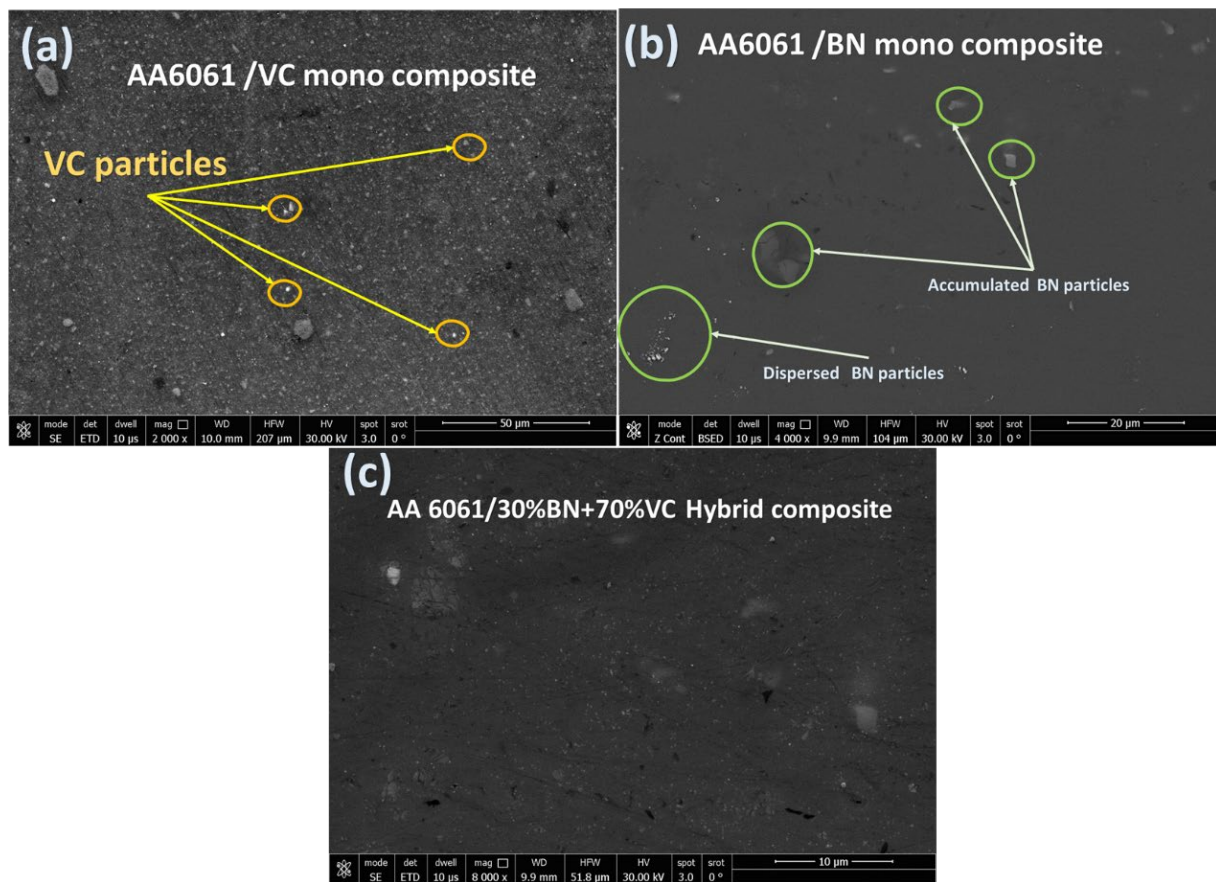
**Figure 5.** Effect of reinforcement particles volume fraction on grain refinement in aluminum alloy AA6061 composites matrices.

Figure 6 shows the scanning electron microscopy (SEM) image exhibiting a homogeneous distribution of (BN) and (VC) particles within the AA 6061 alloy matrix for the mono- and hybrid-composite matrices. The equal distribution of reinforcing particles throughout the composite is crucial for attaining favorable mechanical properties. This ensures that the particles are neither clustered nor conglomerated. The uniform dispersion of the reinforcing particles may be ascribed to the production approach utilized in fabricating the composite material. This procedure has the potential to disperse agglomerates of reinforcement particles and achieve a uniform distribution throughout the matrix [36]. The even distribution of reinforcing particles offers numerous advantages. Initially, enhancing the mechanical properties of the composite can be achieved by introducing additional barriers to hinder the spread of cracks. Additionally, it contributes to the enhancement of the structural integrity of the composite material by inhibiting the development of significant fractures.



**Figure 6.** SEM image of (a) AA 6061/VC mono composite, (b) AA 6061/BN mono composite, and (c) AA 6061/30%BN+70%VC hybrid composite fabricated using friction stir processing.

### 3.2. Electrical Property

The electrical conductivity of the aluminum alloy AA 6061 in its pure form is estimated to be around  $2.76 \times 10^7$  S/m. This study incorporated semiconductor vanadium carbide and insulating boron nitride particles into a composite matrix to investigate their effects in both single and hybrid forms. The enhanced electrical conductivity of vanadium carbide compared to boron nitride can be attributed to its greater abundance of free electrons, which facilitate the flow of electric current. VC has semiconductor properties, while boron nitride demonstrates insulating characteristics. VC has a narrow band gap, facilitating electron movement between different energy levels. The increased mobility of electrons leads to an elevated level of electrical conductivity [37].

Moreover, it is worth noting that vanadium carbide exhibits a larger density of free electrons than boron nitride. This phenomenon is attributed to the elevated quantity of valence electrons present in vanadium carbide. Valence electrons refer to the electrons occupying the outermost electron shell of an atom. These electrons exhibit a higher likelihood of engaging in electrical conduction. The incorporation of vanadium carbide particles into the aluminum alloy resulted in an enhancement of its electrical conductivity, but still less than the FSPed of the base metal, as shown in Figure 7. The composite material AA 6061/30%BN+70%VC had the highest level of electrical conductivity, measuring around  $2.08 \times 10^7$  S/m.

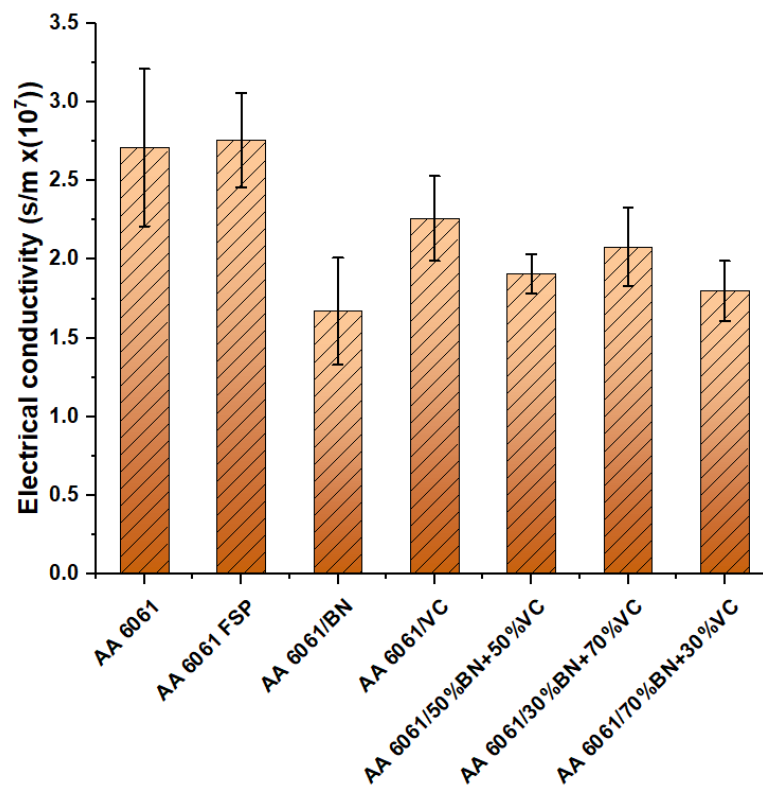
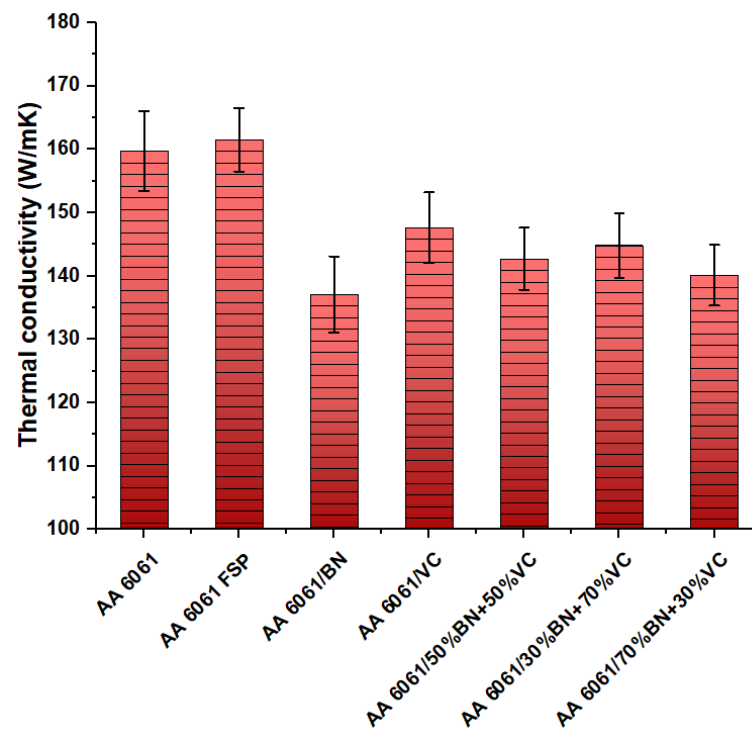


Figure 7. Electrical conductivity of the investigated samples.

Multiple elements play a role in the augmentation of electrical conductivity observed in composite metal matrix materials. One contributing element is the heightened abundance of unbound electrons that are readily available to facilitate the flow of electric current. The presence of reinforcement particles can offer supplementary locations for electron scattering, augmenting the population of free electrons that are accessible for the conduction of electrical current. Another contributing element is the enhanced electrical connectivity between the reinforcing particles and the aluminum matrix [38]. The accomplishment of this objective can be realized through the application of an appropriate interface coating on the reinforcing particles. The augmentation in electrical conductivity exhibited by these composite metal matrix materials holds significant advantages for various applications. Enhancing the electrical contact between the reinforcement particles and the aluminum matrix is important, especially in composite materials with larger volume fractions of reinforcement particles. The presence of reinforcement particles within these materials enables the formation of a network structure, hence impeding the flow of electric current across the matrix.

### 3.3. Thermal Conductivity

The data presented in Figure 8 indicates a decrease in the thermal conductivity of metal matrix composites with the incorporation of (BN) particles. In contrast, an increase in thermal conductivity was observed with (VC) particles. The composite material AA 6061/VC had the maximum thermal conductivity. The thermal conductivity of a substance refers to its capacity to conduct thermal energy. (BN) exhibits low thermal conductivity, whereas (VC) demonstrates high thermal conductivity. This phenomenon can be attributed to the decrease in thermal conductivity of metal matrix composites upon incorporating BN particles and, conversely, the rise in thermal conductivity upon adding VC particles. The incorporation of (BN) particles into the metal matrix has the potential to impede the thermal conductivity of the material. This phenomenon can be attributed to the significantly higher density of BN particles than the metal matrix.



**Figure 8.** Thermal conductivity of the investigated samples.

In contrast, the incorporation of VC particles has the potential to enhance the thermal conductivity of the material. This phenomenon can be attributed to the high thermal conductivity shown by VC particles, which facilitates the establishment of a highly interconnected network of heat flow pathways.

The superior thermal conductivity of metal matrix composites (MMCs) with (VC) reinforcements can indirectly contribute to enhanced strength via plastic deformation, particularly grain refinement. Grain refinement is a microstructural modification process that involves reducing the average grain size of a material. This reduction in grain size hinders the movement of dislocations, the crystal defects responsible for plastic deformation, leading to increased strength and hardness. VC reinforcements can promote grain refinement in MMCs through various mechanisms:

- Nucleation: VC particles can act as nucleation sites for grain formation during solidification, leading to a finer grain structure;
- Zener pinning: VC particles can pin grain boundaries, preventing grain growth during subsequent heat treatments;
- Particle-induced dislocation generation: The mismatch in crystal structure and lattice parameters between VC particles and the metal matrix can induce dislocation generation, hindering grain growth.

The enhanced thermal conductivity of VC-reinforced MMCs plays a role in grain refinement by facilitating heat dissipation during solidification and subsequent heat treatments. Efficient heat dissipation promotes uniform temperature distribution, minimizing thermal stresses and preventing excessive grain growth.

The specific temperature range for grain refinement depends on the specific MMC system and the desired degree of grain refinement. In general, grain refinement occurs at temperatures below the recrystallization temperature of the metal matrix. For AA6061 aluminum, the recrystallization temperature typically lies between 450 °C and 500 °C. Therefore, grain refinement processes for AA6061/VC MMCs are typically conducted within this temperature range.

The thermal conductivity of a hybrid composite is contingent upon the volume fraction of (BN) and (VC) particles present inside the composite. Enhancing thermal conductivity

in metal matrix composites can yield advantages across several applications. For instance, these materials can produce heat sinks, thermal interface materials, and electronic packaging materials. Heat sinks are employed to dissipate heat generated by electronic devices, while thermal interface materials are utilized to enhance heat transfer efficiency between two surfaces. Additionally, electronic packaging materials safeguard electronic equipment against the detrimental effects of excessive heat.

### 3.4. Mechanical Properties

The compressive strength results showed that all the composites tested had higher compressive strength than the base alloy AA 6061 (Figure 9). The hybrid composites with BN and VC reinforcements had the highest compressive strength, followed by the mono composites with BN and VC alone. The hybrid composite with a 30% BN and 70% VC reinforcement content had the highest compressive strength of all the composites tested. The improved compressive strength of the hybrid composites is likely due to the synergistic effects of the two reinforcements. BN is a hard and brittle material, while VC is a soft and tough material. Combining these two materials can provide a composite with high strength and toughness. The observed enhancements in compressive strength of the composites, relative to the parent alloy AA6061, varied between 18.1% and 31.7% (Table 3). This finding implies that the application of reinforcement techniques involving BN, VC, or a combination of both can lead to a substantial enhancement in the compressive strength of AA 6061. The hybrid composite consisting of 30% BN and 70% VC reinforcement content exhibited the most substantial percentage improvement, amounting to 25.8%. This observation implies that, as mentioned earlier, the hybrid composite exhibits considerable potential for use in scenarios that demand elevated compressive strength. The mono composite reinforced with VC exhibited the most substantial percentage improvement, reaching 31.7%. This implies that VC might be a more productive reinforcement for enhancing compressive strength than BN. Nevertheless, it is crucial to acknowledge that the hybrid composite, including 30% BN and 70% VC reinforcement content, exhibited a greater compressive strength than the mono composite reinforced only with VC. This observation implies that the combined impacts of BN and VC can potentially enhance the composite material's compressive strength to a greater extent. In summary, the findings of this investigation indicated that the utilization of BN and VC reinforcements in hybrid composites holds significant potential in developing lightweight and high-strength materials. These materials are particularly well-suited for applications that involve substantial compressive loading.

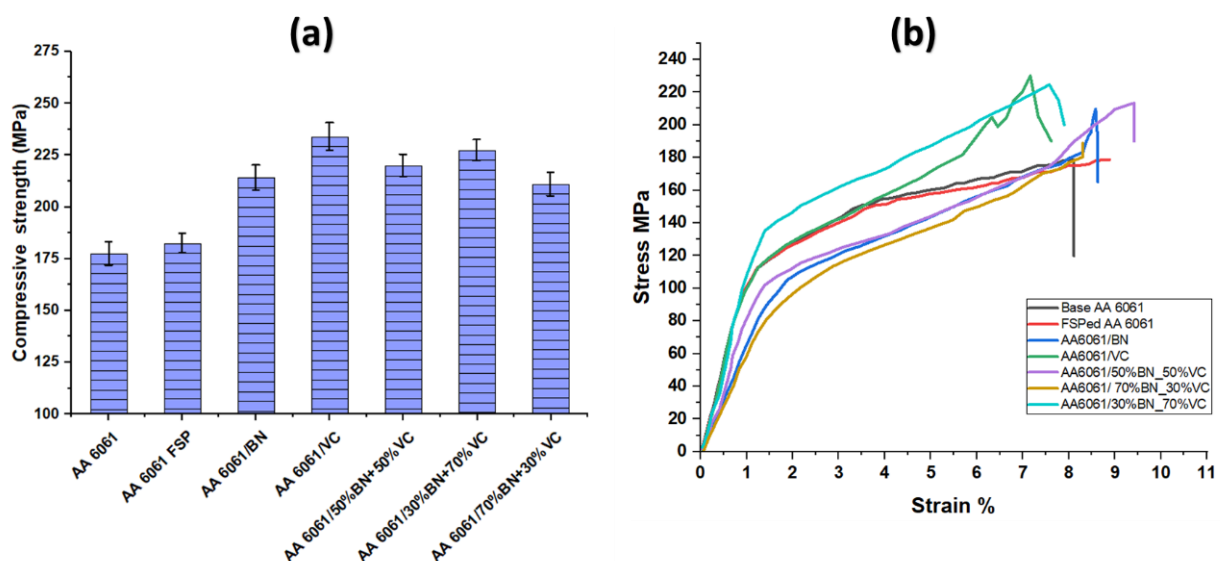


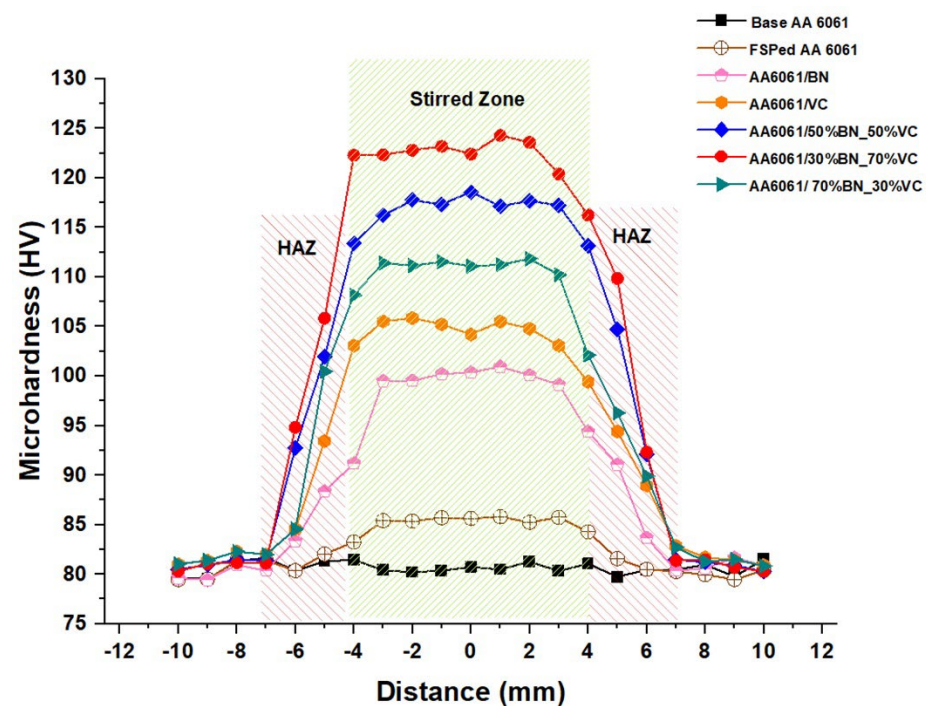
**Figure 9.** (a) Comparative compressive strength of AA 6061 and their composites, (b) stress–strain curve of the investigated samples.

**Table 3.** Percentage of improvement in the compressive strength of the mono and hybrid composites with respect to the base alloy AA6061.

Composite	Percentage Improvement
AA 6061/BN	21.60%
AA 6061/VC	31.70%
AA 6061/50%BN+50%VC	23.10%
AA 6061/30%BN+70%VC	25.80%
AA 6061/70%BN+30%VC	18.10%

### 3.5. Microhardness Profile

The microhardness profile of the analyzed sample is depicted in Figure 10. It is evident from the figure that the microhardness of all composite samples surpassed that of the wrought AA 6061 alloy. The observed phenomenon can be attributed to reinforcing particles within the composite samples. The microhardness of the composite samples had a negative correlation with the distance from the composite surface, indicating a reduction in hardness as the distance increases. The observed phenomenon can be attributed to the positive correlation between the distance from the composite surface and the grain size of the composite material. The microhardness values of the hybrid composite samples were found to be the highest. The hybrid composite samples consisted of BN and VC particles, which exhibited enhanced capability in impeding grain development and dislocation movement. The microhardness value of the mono-composite AA6061/VC sample was greater than that of the mono-composite AA6061/BN sample. This disparity can be attributed to the inherent difference in hardness between VC and BN. The microhardness value of the hybrid-composite 50%BN\_50%VC sample was comparatively higher than that of the hybrid-composite 30%BN\_70%VC sample and the hybrid-composite 70%BN\_30%VC sample. An equal proportion of BN and VC particles in the 50%BN\_50%VC sample probably contributed to its enhanced ability to impede grain development and dislocation movement.

**Figure 10.** Profile of the microhardness of samples of base metal, mono composites, and hybrid composites produced via friction stir processing.

The microhardness profile of the hybrid-composite sample AA6061/30%BN\_70%VC exhibited a greater degree of symmetry compared to the microhardness profiles observed in the remaining composite samples. This hypothesis is plausible due to the higher proportion of VC particles in the AA6061/30%BN\_70%VC sample, which exhibited a more homogeneous distribution throughout the matrix. In general, the findings from the microhardness profile analysis indicate that the friction stir processing (FSP) technique is a viable method for producing AA 6061 alloy and its composites, as it yields various microhardness values. The microhardness of the material can be modified by manipulating the composition and quantity of the reinforcing particles employed. The consequences of the microhardness profile results are significant to the design and development of AA 6061 alloy and its composites. The findings indicate that hybrid composite samples containing an equal proportion of BN and VC particles can yield materials with the highest microhardness values.

The hybrid composite with a 30% BN and 70% VC reinforcement content had the highest compressive strength of all the composites tested. This is likely due to the synergistic effects of the two reinforcements. BN is a hard and brittle material, while VC is a soft and tough material. Combining these two materials can provide a composite with high strength and toughness. A hybrid composite with a 30% BN and 70% VC reinforcement content also had the highest microhardness of all the composites tested. This is because the VC particles are harder than the BN particles and are more effective at pinning dislocations. Based on the results of this study, the current study recommends using a hybrid composite with a 30% BN and 70% VC reinforcement content for applications that require both high compressive strength and high microhardness. However, if you are only concerned with compressive strength, then a mono composite with VC alone may be sufficient.

#### 4. Conclusions

This study comprehensively investigated the impact of incorporating BN and VC reinforcements on the properties of FSPed AA6061 alloy composites.

- The findings revealed that VC exhibits superior grain refining capabilities compared to BN, with hybrid composites containing finer BN particles demonstrating the smallest grain size. Hence, the synergistic combination of VC and BN could serve as an optimal approach for grain structure refinement in AA6061 alloy through FSP.
- The incorporation of BN particles in metal matrix composites generally leads to a reduction in both thermal and electrical conductivity, while the addition of VC particles enhances both properties. The AA6061/VC composite exhibited the highest thermal conductivity among all tested composites, making it a promising candidate for efficient heat dissipation applications. The hybrid-composite AA6061/30%BN+70%VC demonstrated remarkable electrical conductivity, with a mere 2.8% reduction compared to the base alloy AA6061. Additionally, the mono-composite AA6061/VC exhibited only a 7.5% decrease in thermal conductivity compared to AA6061, highlighting the potential of VC reinforcement to maintain electrical and thermal properties.
- The composite material comprising 30% BN and 70% VC reinforcement surpassed all other tested composites in compressive strength. The observed enhancement in compressive strength for mono and hybrid composites ranged from 17.1% to 31.5% compared to the parent AA6061 alloy. These findings demonstrate that reinforcement using BN, VC, or a combination of both materials can significantly improve the compressive strength of AA6061.

**Author Contributions:** Conceptualization, E.B. and F.D.; methodology, E.B.M.; software, E.E.; validation, E.B. and F.D.; formal analysis, A.A.; investigation, E.B.M.; writing—original draft preparation, E.B.; writing—review and editing, E.B.M.; supervision, S.S.M. All authors have read and agreed to the published version of the manuscript.

**Funding:** This research was funded by Ministry of Education and King Abdulaziz University, in Saudi Arabia, grant number [IFPRC-64-135-2020].

**Data Availability Statement:** Data is contained within the article.

**Acknowledgments:** The authors extend their appreciation to the Deputyship of Research & Innovation, Ministry of Education in Saudi Arabia, for funding this research work through project number (IFPRC-64-135-2020) and the King Abdulaziz University, Jeddah, Saudi Arabia.

**Conflicts of Interest:** The authors declare no conflict of interest.

## References

1. Branco, R.; Berto, F.; Kotousov, A. Mechanical Behaviour of Aluminium Alloys. *Appl. Sci.* **2018**, *8*, 146. [[CrossRef](#)]
2. Varshney, D.; Kumar, K. Application and use of different aluminium alloys with respect to workability, strength and welding parameter optimization. *Ain Shams Eng. J.* **2021**, *12*, 1143–1152. [[CrossRef](#)]
3. Sarvaiya, J.; Singh, D. Development of surface composites AA5052/SiC using micro and nano-SiC reinforcement particles via friction stir processing. *Mater. Today Proc.* **2023**, *in press*. [[CrossRef](#)]
4. Khalid, M.Y.; Umer, R.; Khan, K.A. Review of recent trends and developments in aluminium 7075 alloy and its metal matrix composites (MMCs) for aircraft applications. *Results Eng.* **2023**, *20*, 101372. [[CrossRef](#)]
5. Keneshloo, M.; Paidar, M.; Taheri, M. Role of SiC ceramic particles on the physical and mechanical properties of Al–4%Cu metal matrix composite fabricated via mechanical alloying. *J. Compos. Mater.* **2016**, *51*, 1285–1298. [[CrossRef](#)]
6. Mehdi, H.; Mishra, R.S. Effect of multi-pass friction stir processing and SiC nanoparticles on microstructure and mechanical properties of AA6082-T6. *Adv. Ind. Manuf. Eng.* **2021**, *3*, 100062. [[CrossRef](#)]
7. Bhanuprakash, L.; Thejasree, P.; John, F.; Prabha, R. Study on mechanical and micro-structural properties of aluminium matrix composite reinforced with graphite and granite fillers. *Mater. Today Proc.* **2023**, *in press*. [[CrossRef](#)]
8. Abushanab, W.S.; Moustafa, E.B.; Goda, E.S.; Ghandourah, E.; Taha, M.A.; Mosleh, A.O. Influence of Vanadium and Niobium Carbide Particles on the Mechanical, Microstructural, and Physical Properties of AA6061 Aluminum-Based Mono- and Hybrid Composite Using FSP. *Coatings* **2023**, *13*, 142. [[CrossRef](#)]
9. Hynes, N.R.J.; Raja, S.; Tharmaraj, R.; Pruncu, C.I.; Dispinar, D. Mechanical and tribological characteristics of boron carbide reinforcement of AA6061 matrix composite. *J. Braz. Soc. Mech. Sci. Eng.* **2020**, *42*, 155. [[CrossRef](#)]
10. Sharma, D.K.; Patel, V.; Badheka, V.; Mehta, K.; Upadhyay, G. Different reinforcement strategies of hybrid surface composite AA6061/(B<sub>4</sub>C+MoS<sub>2</sub>) produced by friction stir processing. *Mater. Und Werkst.* **2020**, *51*, 1493–1506. [[CrossRef](#)]
11. Ammal, M.A.; Sudha, J. Microstructural Evolution & Mechanical Properties of ZrO<sub>2</sub>/GNP and B<sub>4</sub>C/GNP reinforced AA6061 Friction Stir Processed Surface Composites—A Comparative study. *Proc. Inst. Mech. Eng. Part B J. Eng. Manuf.* **2022**, *237*, 1149–1160.
12. Moustafa, E.B. Hybridization effect of BN and Al<sub>2</sub>O<sub>3</sub> nanoparticles on the physical, wear, and electrical properties of aluminum AA1060 nanocomposites. *Appl. Phys. A* **2021**, *127*, 724. [[CrossRef](#)]
13. Porz, L.; Klomp, A.J.; Fang, X.; Li, N.; Yildirim, C.; Detlefs, C.; Bruder, E.; Höfling, M.; Rheinheimer, W.; Patterson, E.A.; et al. Dislocation-toughened ceramics. *Mater. Horiz.* **2021**, *8*, 1528–1537. [[CrossRef](#)]
14. Nautiyal, P.; Bustillos, J.; Selvam, T.; Zhang, C.; Seal, S.; Boesl, B.; Agarwal, A. In Situ Investigation of Deformation Mechanisms Induced by Boron Nitride Nanotubes and Nanointerphases in Ti–6Al–4V Alloy. *Adv. Eng. Mater.* **2022**, *24*, 2200610. [[CrossRef](#)]
15. Netto, N.; Zhao, L.; Soete, J.; Pyka, G.; Simar, A. Manufacturing high strength aluminum matrix composites by friction stir processing: An innovative approach. *J. Mater. Process. Technol.* **2020**, *283*, 116722. [[CrossRef](#)]
16. Bayazid, S.M.; Farhangi, H.; Ghahramani, A. Investigation of Friction Stir Welding Parameters of 6063-7075 Aluminum Alloys by Taguchi Method. *Procedia Mater. Sci.* **2015**, *11*, 6–11. [[CrossRef](#)]
17. Boopathi, S.; Jeyakumar, M.; Singh, G.R.; King, F.L.; Pandian, M.; Subbiah, R.; Haribalaji, V. An experimental study on friction stir processing of aluminium alloy (AA-2024) and boron nitride (BNp) surface composite. *Mater. Today Proc.* **2022**, *59*, 1094–1099. [[CrossRef](#)]
18. Penchal Reddy, M.; Manakari, V.; Parande, G.; Ubaid, F.; Shakoore, R.; Mohamed, A.; Gupta, M. Enhancing compressive, tensile, thermal and damping response of pure Al using BN nanoparticles. *J. Alloys Compd.* **2018**, *762*, 398–408. [[CrossRef](#)]
19. Hashim, F.A.; Abdulkader, N.J.; Jasim, N.S. Effect of Nano BN Addition on the Properties of an Aluminum Metal Matrix Composite. *Eng. Technol. J.* **2018**, *36*, 691–695. [[CrossRef](#)]
20. Wie, J.; Kim, K.; Kim, J. High thermal conductivity composites obtained by novel surface treatment of boron nitride. *Ceram. Int.* **2020**, *46 Part A*, 17614–17620. [[CrossRef](#)]
21. Irshad, H.M.; Farooq, A.; Hakeem, A.S.; Azeem, M.Z.; Ehsan, M.A. Electrochemical study of aluminum–cubic boron nitride composites synthesized via spark plasma sintering for engineering applications. *J. Alloys Compd.* **2023**, *965*, 171210. [[CrossRef](#)]
22. Ruh, R.; Donaldson, K.Y.; Hasselman, D.P.H. Thermal Conductivity of Boron Carbide–Boron Nitride Composites. *J. Am. Ceram. Soc.* **1992**, *75*, 2887–2890. [[CrossRef](#)]
23. Kheirkhah, S.; Imani, M.; Aliramezani, R.; Zamani, M.H.; Kheilnejad, A. Microstructure, mechanical properties and corrosion resistance of Al6061/BN surface composite prepared by friction stir processing. *Surf. Topogr. Metrol. Prop.* **2019**, *7*, 035002. [[CrossRef](#)]
24. Bisht, A.; Kumar, V.; Li, L.H.; Chen, Y.; Agarwal, A.; Lahiri, D. Effect of warm rolling and annealing on the mechanical properties of aluminum composite reinforced with boron nitride nanotubes. *Mater. Sci. Eng. A* **2018**, *710*, 366–373. [[CrossRef](#)]

25. Wu, B.; Ibrahim, M.; Raja, S.; Yusof, F.; Razak, B.B.A.; Bin Muhamad, M.R.; Huang, R.; Zhang, Y.; Badruddin, I.A.; Hussien, M.; et al. The influence of reinforcement particles friction stir processing on microstructure, mechanical properties, tribological and corrosion behaviors: A review. *J. Mater. Res. Technol.* **2022**, *20*, 1940–1975. [[CrossRef](#)]
26. Palanivel, R.; Dinaharan, I.; Laubscher, R.F.; Davim, J.P. Influence of boron nitride nanoparticles on microstructure and wear behavior of AA6082/TiB<sub>2</sub> hybrid aluminum composites synthesized by friction stir processing. *Mater. Des.* **2016**, *106*, 195–204. [[CrossRef](#)]
27. Srinivas, K.S.; Mohan, M.M. Experimental Investigation of Mechanical Properties of Ceramic Reinforced Al-7075 Metal Matrix Hybrid Composites. *Mater. Sci. Forum* **2020**, *979*, 34–39. [[CrossRef](#)]
28. Ghasali, E.; Pakseresht, A.H.; Alizadeh, M.; Shirvanimoghaddam, K.; Ebadzadeh, T. Vanadium carbide reinforced aluminum matrix composite prepared by conventional, microwave and spark plasma sintering. *J. Alloys Compd.* **2016**, *688*, 527–533. [[CrossRef](#)]
29. Wang, J.; Fu, S.J.; Ding, Y.C.; Wang, Y.S. Study on Microstructure of Vanadium and Chromium-Carbide Reinforced Fe Matrix Surface Composite. *Adv. Mater. Res.* **2012**, *399–401*, 425–429. [[CrossRef](#)]
30. Zhong, L.; Ye, F.; Xu, Y.; Li, J. Microstructure and abrasive wear characteristics of in situ vanadium carbide particulate-reinforced iron matrix composites. *Mater. Des. (1980–2015)* **2014**, *54*, 564–569. [[CrossRef](#)]
31. Jung, J.-H.; Lee, S.-J.; Kim, H.-S. Estimation of Average Grain Size from Microstructure Image Using a Convolutional Neural Network. *Materials* **2022**, *15*, 6954. [[CrossRef](#)] [[PubMed](#)]
32. Abdel Aziz, S.S.; Abulkhair, H.; Moustafa, E.B. Role of hybrid nanoparticles on thermal, electrical conductivity, microstructure, and hardness behavior of nanocomposite matrix. *J. Mater. Res. Technol.* **2021**, *13*, 1275–1284. [[CrossRef](#)]
33. Wang, W.; Yuan, S.; Qiao, K.; Wang, K.; Zhang, S.; Peng, P.; Zhang, T.; Peng, H.; Wu, B.; Yang, J. Microstructure and nanomechanical behavior of friction stir welded joint of 7055 aluminum alloy. *J. Manuf. Process.* **2021**, *61*, 311–321. [[CrossRef](#)]
34. Reza-E-Rabby, M.; Olszta, M.J.; Overman, N.R.; McDonnell, M.; Whalen, S.A. Friction stir dovetailing of AA7099 to steel with AA6061 interlayer for reduced Zn embrittlement at dissimilar interface. *J. Manuf. Process.* **2021**, *61*, 25–34. [[CrossRef](#)]
35. Ahmed, H.M.; Ahmed, H.A.M.; Hefni, M.; Moustafa, E.B. Effect of Grain Refinement on the Dynamic, Mechanical Properties, and Corrosion Behaviour of Al-Mg Alloy. *Metals* **2021**, *11*, 1825. [[CrossRef](#)]
36. Rathee, S.; Maheshwari, S.; Siddiquee, A.N.; Srivastava, M. Distribution of reinforcement particles in surface composite fabrication via friction stir processing: Suitable strategy. *Mater. Manuf. Process.* **2018**, *33*, 262–269. [[CrossRef](#)]
37. Alsorujji, G.; Moustafa, E.B.; Alzahrani, M.A.; Taha, M.A. Preparation of Silicon Bronze-Based Hybrid Nanocomposites with Excellent Mechanical, Electrical, and Wear Properties by Adding the Ti<sub>3</sub>AlC<sub>2</sub> MAX Phase and Granite Via Powder Metallurgy. *Silicon* **2023**, *15*, 2753–2763. [[CrossRef](#)]
38. Ashrafi, N.; Ariff, A.H.M.; Jung, D.-W.; Sarraf, M.; Foroughi, J.; Sulaiman, S.; Hong, T.S. Magnetic, Electrical, and Physical Properties Evolution in Fe<sub>3</sub>O<sub>4</sub> Nanofiller Reinforced Aluminium Matrix Composite Produced by Powder Metallurgy Method. *Materials* **2022**, *15*, 4153. [[CrossRef](#)]

**Disclaimer/Publisher’s Note:** The statements, opinions and data contained in all publications are solely those of the individual author(s) and contributor(s) and not of MDPI and/or the editor(s). MDPI and/or the editor(s) disclaim responsibility for any injury to people or property resulting from any ideas, methods, instructions or products referred to in the content.